Twenty-Seventh Symposium (International) on Combustion/The Combustion Institute, 1998/pp. 2477–2483

SPATIAL DISTRIBUTIONS OF H, CN, AND C_2 IN A DIAMOND-GROWING OXYACETYLENE FLAME

R. J. H. KLEIN-DOUWEL AND J. J. TER MEULEN
Applied Physics
University of Nijmegen
Toernooiveld, 6525 ED Nijmegen, The Netherlands

Two-dimensional laser-induced fluorescence (2D-LIF) measurements are applied to the chemical vapor deposition (CVD) of diamond by an oxyacetylene flame to visualize the distributions of atomic hydrogen, C_2, and CN in the gas phase during diamond growth. Experiments are carried out in laminar flames and reveal that atomic hydrogen is ubiquitous at and beyond the flame front. Its presence extends to well outside the diamond deposition region, whereas the C_2 distribution is limited to the flame front and the acetylene feather. CN is found to be present mostly at the outer edge of the flame, where ambient air interacts with flame gases. The diamond layers obtained are characterized by optical as well as scanning electron microscopy (SEM) and cathodoluminescence topography (CL). Clear relations are observed between the local variations in growth rate of the diamond layer and the distribution of H, C_2, and CN in the boundary layer just above the substrate. Further relations between CN and the morphology and the nitrogen incorporation as identified by CL of the deposited diamond layer are found as well. These relations agree with theoretical models describing the importance of the mentioned species in (flame) deposition processes of diamond. Three separate regions can be discerned in the flame and the diamond layer, where the gas phase and diamond growth are predominantly governed by the flame source gases, the ambient atmosphere, and the interaction of both, respectively.

Introduction

A relatively simple method to make sufficient amounts of radicals for chemical vapor deposition (CVD) of diamond is the use of highly exothermic reactions that take place in, for instance, flames. This idea was first utilized by Hirose in 1988, who employed an oxyacetylene combustion flame to deposit diamond on a cooled substrate under atmospheric conditions [1]. This method was soon picked up by several other groups, and the technique is now well developed to deposit polycrystalline diamond on nondiamond substrates and single crystalline diamond layers on a diamond seed crystal [2–6], which is either of natural origin or grown by another CVD technique.

The commercially available welding torch used in this work yields a laminar, conical oxyacetylene flame, which impinges at normal incidence on the cooled substrate. Premixed flat flames have also been used for diamond deposition, but in general, this results in lower diamond growth rates [7–9]. Assuming chemical equilibrium in the gas phase, its composition can be calculated from the flame feed gases, which shows CO, H_2, H, and C_2H_2 to be the major species beyond the flame front [10–12]. These results are given only for one fixed set of deposition conditions, but recently, species and temperature profiles and the corresponding diamond growth rate and quality have been calculated for various sets of growth conditions in the laminar oxyacetylene flame, agreeing reasonably well with empirical results [13,14].

The mechanism of the diamond growth process on the surface is in general thought to be the following: the surface is covered by free sites and adsorbed hydrogen atoms, the latter of which can be etched away by gas-phase hydrogen atoms. At the resulting free site, CH_3, thought to be an important growth species, can adsorb. CN and OH, if present, are considered to be important as well for hydrogen abstraction from the surface. Apart from CH_3, the growth species may include CH, C_2, and CN, molecules often present in flames.

The exact deposition mechanism, however, is not well known, and the two-dimensional laser-induced fluorescence (LIF) technique is used to obtain relations between the gas phase and the diamond-layer characteristics, such as growth rate, morphology, and nitrogen incorporation. The LIF method is applied because of its species specificity, high spatial resolution, nonintrusiveness, and high sensitivity. In combination with a pulsed laser and a charge coupled device (CCD) camera, laminar flames are studied in detail. The obtained information elucidates the role of flame species and their importance (or unimportance) for diamond growth. The relations between diamond growth and flame characteristics

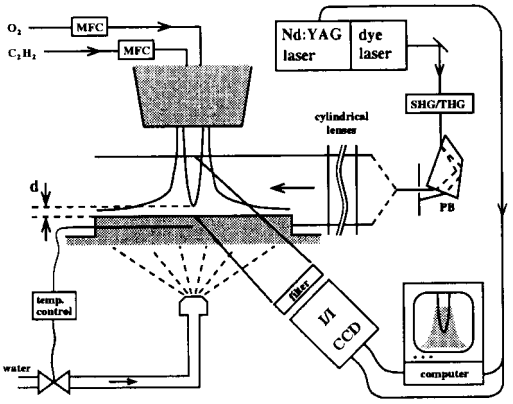

FIG. 1. Schematic representation of the diamond growth and LIF detection setup. MFC = mass flow controllers, SHG/THG = second/third harmonic generation (if applicable), PB = Pellin-Broca prism, I/I = image intensifier, CCD = charge coupled device camera. The distance d between the substrate and the tip of the flame front is indicated.

can be used as a monitor in the growth process, enabling fast feedback to obtain diamond layers with properties closer to desired for industrial applications, and reveal which parameters are important for upscaling the deposition area, another (economic) aspect of industrial application of flame growth of diamond.

Experimental Setup: Diamond Growth

The experimental setup for diamond growth combined with LIF detection during deposition is depicted in Fig. 1. Exact experimental details are described in previous studies on H, C_2, CH, CN, and OH [15–17], but important parameters and their typical values are given here. The acetylene supersaturation S_{ac} is important during diamond deposition, which is why both the oxygen and acetylene flows are regulated by mass flow controllers. S_{ac} = 0% for the neutral flame (neither fuel-rich nor oxygen-rich) and $S_{ac} > 0\%$ in a fuel-rich flame, in which case the so-called acetylene feather is formed outside the flame front. The burner orifice diameter is 1.4 mm, and the oxygen flow is 3.0 standard liters per minute (SLM). Diamond growth can take place on the substrate, positioned in the acetylene feather, for $0 < S_{ac} \lesssim 9\%$. For $S_{ac} \gtrsim 9\%$, the deposit will not contain diamond anymore but mostly amorphous carbon. In most experiments, S_{ac} = 5% is used, resulting in an acetylene flow of ≈2.5 SLM.

The substrate consists of a thin (0.5 mm) molybdenum square soldered to a molybdenum holder. The substrate is cooled from below by a pulsed water nozzle, which is regulated by a thermocouple located 2.5 mm beneath the center of the substrate surface. The thermocouple temperature T_s is kept at 900 ± 1 °C, resulting in a deposition temperature T_d at the substrate surface of 1050 ± 20 °C. Prior to deposition, the molybdenum substrate is scratched with micrometer-sized diamond powder to enhance nucleation and adhesion to the substrate of the diamond layer to be grown.

Apart from S_{ac} and T_d, the distance d between the tip of the flame front and the substrate (indicated in Fig. 1) is a main parameter in determining the characteristics of the obtained diamond layer. Typical values of d are between 0.5 and 3 mm, where short distances result in a high central maximum in the diamond growth rate v_d (which can be more than 150 μm/h), and larger distances yield a central valley surrounded by an annulus of enhanced growth. Diamond layers deposited at a distance d of 1 to 2 mm reveal in their center a continuous area of uniform thickness and well-connected randomly oriented {111} and {100} facets. The diameter of this region is 4–5 mm. At distances d larger than about 3 mm, a so-called core zone [18] of ≈2.0 mm ϕ develops in the center. In this core zone, the crystallites mainly reveal {111} facets and are often much smaller than in the rest of the center. This is shown in Fig. 2a: The large crystallites in this photograph, which are of normal size, are interspersed with many much smaller ones, and they also exhibit a large amount of secondary nucleation.

Outside the center, an annular region of enhanced growth is observed, where the morphology is markedly different. This annulus typically exhibits large columnar crystallites, separated by voids or embedded in an amorphous layer, which frequently have {100} top facets almost parallel to the substrate. Outside the annulus of enhanced growth, a sharp transition zone is generally found, which is only 0.1–0.2 mm wide and can exhibit a continuous, highly {100} textured morphology. A photograph of this is shown in Fig. 2b.

Morphologies like this are of interest to many applications of polycrystalline diamond layers. Beyond this transition zone, the morphology resembles that of the central area, with the size of the crystallites rapidly diminishing toward the edge of the diamond layer.

After growth, the deposited diamond layers are characterized by optical differential interference contrast microscopy (DICM), scanning electron microscopy (SEM), Raman spectroscopy, and cathodoluminescence topography (CL), which is a technique that reveals information about the incorporation of nitrogen into the diamond layer. The diamond-layer thickness is determined by focusing the optical microscope with an accuracy of ±2 μm at different locations of the layer.

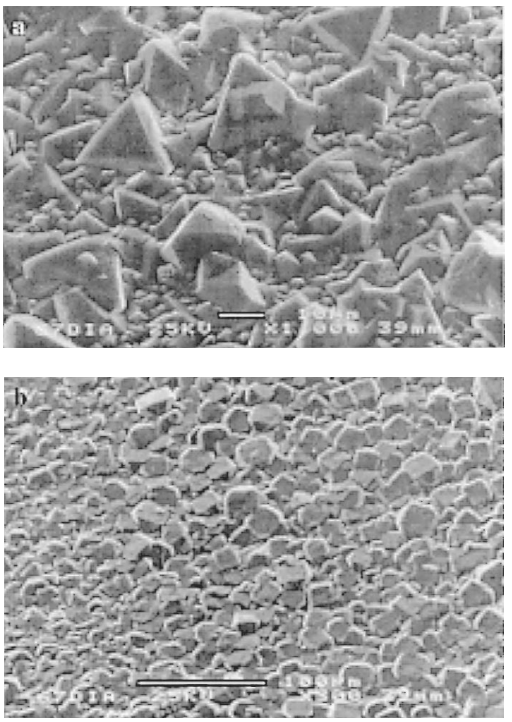

FIG. 2. SEM photographs revealing the morphology of a diamond layer, deposited by a laminar flame at $d = 4.04$ mm. (a) The *core zone,* showing normal-sized crystallites embedded in many much smaller ones. Diamond layers deposited at smaller distances d reveal a continuous central layer of normal-sized crystallites. The scale bar is 10 μm long. (b) Transition zone, revealing a highly {100} textured region, beyond the annulus of enhanced growth (which is located outside the upper right-hand corner of the image). At the left-hand side, the small crystallites of the diamond-layer edge become visible. The scale bar is 100 μm long.

TABLE 1
Species detected by LIF during diamond growth and their excitation wavelengths

Species	Transition	λ_{exc} (nm)
H	$n = 3 \leftarrow n = 1$	2×205
NO	$A^2\Sigma^+(v = 0) \leftarrow X^2\Pi(v'' = 1)$	193
	$A^2\Sigma^+(v' = 2) \leftarrow X^2\Pi(v'' = 0)$	205
OH	$A^2\Sigma^+(v' = 3) \leftarrow X^2\Pi(v'' = 0)$	248
	$A^2\Sigma^+(v' = 1) \leftarrow X^2\Pi(v'' = 0)$	282
	$A^2\Sigma^+(v' = 0) \leftarrow X^2\Pi(v'' = 0)$	308
C_2	$C^1\Pi_g(v' = 2) \leftarrow A^1\Pi_u(v'' = 0)$	340
CN	$B^2\Sigma^+(v' = 1) \leftarrow X^2\Sigma^+(v'' = 0)$	359
CH	$B^2\Sigma^-(v' = 0) \leftarrow X^2\Pi(v'' = 0)$	393
C_2	$d^3\Pi_g(v' = 2) \leftarrow a^3\Pi_u(v'' = 0)$	438
	$d^3\Pi_g(v' = 0) \leftarrow a^3\Pi_u(v'' = 2)$	619
	$d^3\Pi_g(v' = 0) \leftarrow a^3\Pi_u(v'' = 3)$	686

Laser-Induced Fluorescence

Figure 1 depicts how the LIF technique is applied to the oxyacetylene flame during the deposition of diamond. The output of an Nd:YAG pumped dye laser (5-ns pulses) is directed to the flame and passes through a cylindrical telescope, resulting in a vertical laser sheet of 0.3 mm thick and several millimeters high. If necessary, frequency doubling and mixing are applied. Fluorescence is collected by a CCD camera equipped with an image intensifier (typically 20-ns exposure time), with an appropriate filter in front of it, and the signals are processed on a personal computer.

A review of the species detected by LIF in the oxyacetylene flame during diamond growth is given in Table 1. All transitions can be excited by a dye laser, using its second or third harmonic if necessary. Only for NO excitation at 193 nm, a tunable ArF excimer laser is used. The LIF signal is proportional to the population density in the lower state of the species of interest. Quantification of the LIF signal suffers from several problems if the LIF method is used in atmospheric pressure flames. Due to collisions of the excited species with neighboring species in the flame, part of the fluorescence is quenched. The effects of temperature variations within the atmospheric pressure oxyacetylene flame on the LIF signals are complex and are therefore not taken into account in the results described next. But many results given concern relative densities in a layer parallel and close to the substrate, where the temperature is not expected to vary very much. Hence, the conclusions drawn from these results will not be affected much by neglecting temperature effects.

Results and Discussion

The distribution of C_2 in the flame during diamond deposition is shown in Fig. 3a. The distance d between the tip of the flame front and the substrate is 2.80 mm. The laser sheet extends from the substrate to about 2 mm above it. Because the background is subtracted, the flame front (total length $\approx$6 mm) is not visible in Fig. 3a. For ease of reference, however, the natural emission of the flame is converted to isophotes and superimposed on the LIF image. From this figure, it is clear that C_2 is present in the acetylene feather and that the maximum signal is found at the flame front. In the acetylene feather, the C_2 signal is more or less constant, but close to the substrate, it drops markedly and a clear central minimum can be observed.

An example of the CN LIF signal is given in Fig. 3b. If compared to Fig. 3a, it is evident that CN is located at the edge of the acetylene feather and that it is not found at or close to the flame front. This

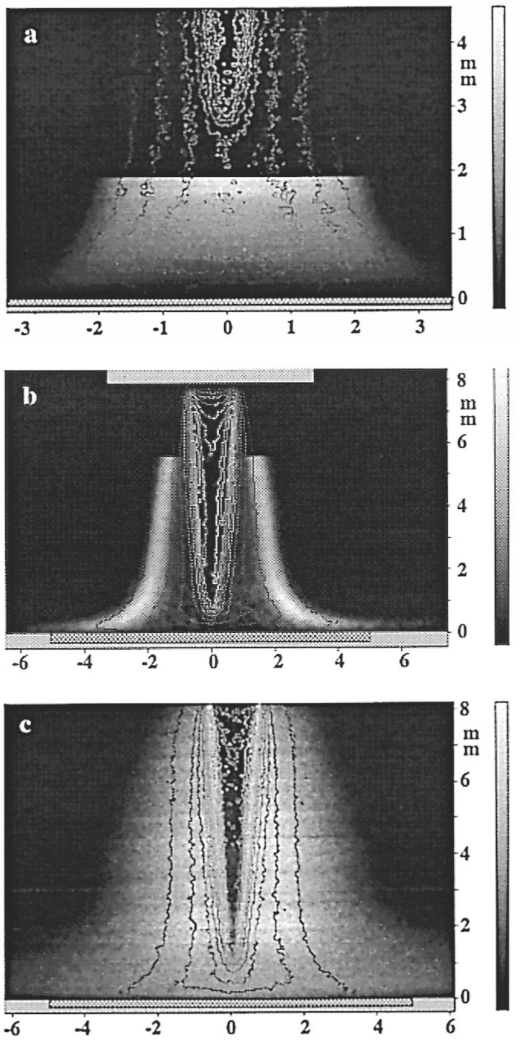

FIG. 3. LIF signals of (a) C_2, (b) CN, and (c) H during diamond deposition in the flame [linear gray scale in arbitrary units, ranging from black (zero) to white (maximum)]. Natural emission of the flame is superimposed (isophotes, representing equal-intensity difference steps). The distance between flame front and substrate is (a) $d = 2.80$ mm, (b) $d = 0.55$ mm, and (c) $d = 0.85$ mm. The images are corrected for the vertical intensity distribution of the laser beam (the noisy uppermost part is removed for reasons of clarity; the H image is constructed from six separate images). The substrate and the burner tip are indicated in gray, the crosshatched area depicts the diamond deposition region, and dimensions are in millimeters.

may be explained by N_2 from the ambient air diffusing into the flame and reacting with carbon-containing species created in the fuel-rich flame.

Figure 3c shows the distribution of the atomic hydrogen LIF signal in nearly the whole flame. Comparison with Figs. 3a and 3b reveals H to be present inside as well as outside the acetylene feather and shows that the H LIF signal is also found at the flame front, where atomic hydrogen is created. It diffuses rapidly throughout the flame and is consumed outside the acetylene feather by reactions with ambient air. The H LIF image is recorded at a relatively small distance of $d = 0.85$ mm, and upon close inspection, a central maximum can be discerned in the LIF signal close to the substrate.

In order to study the species distribution close to the substrate in more detail, horizontal profiles are taken from LIF images obtained at various distances d. Figure 4 shows horizontal profiles of the C_2, CN, and H LIF signals, for each species, one at a relatively small distance d and one at a larger distance. Also shown in this figure is the lateral variation of the growth rate v_d of the corresponding diamond layers, which is measured along the path of the laser beam. The behavior of the H and C_2 profiles is similar: For small distances d, a clear central maximum is found, and the LIF signal decreases more or less linearly with radial distance; and for large distances, the central maximum is replaced by a central minimum, as already discussed. The presence of atomic hydrogen, however, extends radially further than that of C_2.

The general behavior of v_d as a function of d was already discussed. In Fig. 4, the annulus of enhanced growth is clearly visible in the variation of v_d. When v_d is compared to the radial distribution of H LIF signal close to the substrate, it is striking that both show a very similar radial behavior from the center all the way to the edge of the diamond layer, if the annulus of enhanced growth is not taken into account. The good agreement between the H distribution close to the substrate and v_d (apart from the annulus of enhanced growth) indicates the importance of atomic hydrogen to the deposition rate of the diamond layer, which has already been studied elaborately in theory [12,19–22]. The correspondence between the C_2 profiles and v_d is similar to that of atomic hydrogen, although it is limited to a smaller area. The resemblance indicates that C_2 may be important for the diamond growth rate in the center of the deposited layer [15], which agrees to the role of C_2 as a diamond precursor, as put forward by Gruen and coworkers [23–25]. The agreement between the H and C_2 profiles and the behavior of v_d has been observed for other values of d as well [15,17].

Inspection of Fig. 4 shows that v_d drops much less rapidly with increasing distance d in the annulus of enhanced growth than in the center of the diamond

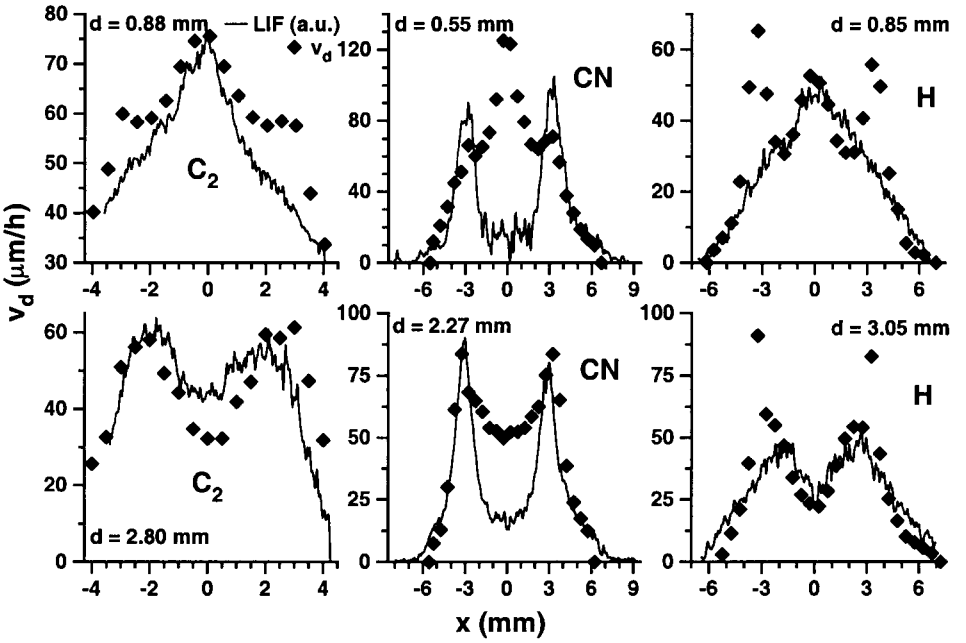

FIG. 4. Horizontal profiles of the C_2 (*left*), CN (*center*), and H (*right*) LIF signals (solid lines) compared to the variation of the growth rate v_d (diamonds) of the corresponding diamond layer, as measured along the path of the laser beam.

layer. In addition to this, the annulus of enhanced growth and the transition zone just outside it reveal a large fraction of {100} facets parallel to the substrate, compared to the center and the outer edge of the diamond layer, as described earlier (see Fig. 2) and in Refs. [5,16,18]. These observations are strong indications that the growth mechanism in the annulus is different from elsewhere in the deposited diamond layer. The fact that the maxima in the horizontal CN profiles coincide with the annulus of enhanced growth (also found for other values of d [16]) therefore indicates that CN or a closely related species (only one or two reaction steps away) may be important in the diamond growth process in the annulus, regarding both the morphology and the local growth rate. The influence of CN (or a closely related species) on the growth rate may be explained by the possibilities of CN and HCN to abstract adsorbed hydrogen from the growing diamond surface [26,27]. The preferential formation of {100} facets parallel to the substrate in and close to the annulus of enhanced growth may also be related to the presence of CN or a closely related species, because similar morphologies have been observed upon nitrogen addition to flame and other diamond-growing CVD systems [26,28–32], studies in which also the positive effect of nitrogen addition to the diamond-growth rate is described.

After growth, the diamond layers are examined by CL to study the incorporation of nitrogen as nitrogen-vacancy pairs into the diamond lattice. Depending on the exact deposition conditions, the nitrogen incorporation in the center of the diamond layer is medium to completely absent, but in the annulus of enhanced growth, a maximum nitrogen incorporation is always found [16,18]. This coincides with the behavior of the CN LIF signals, as previously described.

The amount of reactive nitrogen is maximum at the location where CN is found, that is, above the annulus of enhanced growth. The CN LIF signal can therefore be used as an indicator for nitrogen incorporation into the diamond layer during the flame-growth process. Protecting the flame from ambient nitrogen by an Ar coflow would considerably alter both the flame chemistry in the acetylene feather and the diamond-growth process and is not attempted. Controlled doping of the flame source gases with nitrogen is in progress.

Conclusions

Flame deposition of diamond by the oxyacetylene flame is a relatively simple and fast technique to grow diamond layers on small or curved surfaces. Yet the exact growth mechanism is not well known, and therefore, the LIF method is applied to the flame during diamond growth. Although quantification of the LIF signal is hampered by collisional quenching,

the obtained signals of H, C_2, and CN reveal much information about the diamond-growth process. A strong relation is observed between the distribution of H in the gas-phase boundary layer just above the diamond and the radial variation of the growth rate: the diamond growth rate matches the horizontal distribution of atomic hydrogen very well over the whole deposition area, except for the annulus of enhanced growth. This relation is already expected from theoretical calculations on diamond growth [12,19–22]. The growth rate of the annulus of enhanced growth is about twice what can be expected from the H signal in the gas phase. This can be explained by the presence of CN and related species above the annulus, which have an additional positive effect on the diamond-growth rate.

The horizontal distribution of C_2 just above the central region (≈4 mm diameter) of the growing diamond layer resembles that of atomic hydrogen. A clear relation between C_2 in the gas phase and the growth rate of this central region has been observed. This relation confirms the importance of C_2 as a possible diamond precursor for the central region of the layer, in accordance with theoretical as well as experimental results of Gruen and coworkers [23–25].

The observed relations between H, C_2, and CN and the properties of the obtained diamond layers not only yield information on the growth process but also reveal that their signals are important indicators in the diamond deposition process. In order to adjust the process, the signals can be monitored, to obtain diamond layers with properties closer to desired for (industrial) applications. Whether nitrogen incorporation into the diamond layer is desirable depends on the particular application.

The observed morphology of the deposited diamond layers [5,15,16,18,29,32] and the above-mentioned relations between CN, C_2, and H and the diamond-growth rate, combined with the distribution of OH during diamond deposition (only present outside the acetylene feather [15]), suggest that three separate regions can be distinguished in the gas phase above the diamond layer. The first region is the center of the flame, beyond the flame front, where all species, like C_2, CH, H, H_2, and CH_3, are created by the combustion reactions. Above the growing diamond layer, this central region extends to but does not include the annulus of enhanced growth. The gas-phase composition of this central region determines the properties like growth rate, morphology, and impurity incorporation of the center of the diamond layer. The second region is the rim of the acetylene feather, where the influence of ambient air diffusing into the flame is important. Close to the substrate, this region is limited to the annulus of enhanced growth, whose characteristics are determined by both the flame source gases and the ambient atmosphere. In this region, atomic hydrogen can still be observed. The third region, containing species like OH, H_2O, CO, and CO_2, surrounds the acetylene feather. Diamond growth in this region is restricted by the decreasing carbon and hydrogen concentrations, and the diamond-layer characteristics are less dependent on the flame source gas composition than in the center and the annulus of enhanced growth. All three regions are of interest to diamond growth under the deposition conditions used in the present work, and the LIF method as applied gives direct simultaneous insight into these.

Nomenclature

d	distance between tip of flame front and substrate
S_{ac}	acetylene supersaturation
v_d	diamond-layer growth rate

Acknowledgments

The authors wish to thank Ir. J. J. Schermer, Ir. M. Okkerse, and Dr. W. J. P. van Enckevort for many useful discussions. This work has been made possible by financial support of the Stichting voor Technische Wetenschappen (Technology Foundation).

REFERENCES

1. Hirose, Y. and Kondo, N., *Extended Abstracts, 35th Jpn. Appl. Phys.* Spring Meeting, March 1988, p. 434.
2. Matsui, Y., Yuuki, A., Sahara, M., and Hirose, Y., *Jpn. J. Appl. Phys.* 28:1718 (1989).
3. Janssen, G., van Enckevort, W. J. P., Schaminée, J. J. D., Vollenberg, W., Giling, L. J., and Seal, M., *J. Cryst. Growth* 104:752 (1990).
4. Hanssen, L. M., Snail, K. A., Carrington, W. A., Butler, J. E., Kellogg, S., and Oakes, D. B., *Thin Solid Films* 196:271 (1991).
5. Schermer, J. J., Hogenkamp, J. E. M., Otter, G. C. J., Janssen, G., van Enckevort, W. J. P., and Giling, L. J., *Diamond Rel. Mater.* 2:1149 (1993).
6. Schermer, J. J. and Giling, L. J., *J. Appl. Phys.* 78:2376 (1995).
7. Murayama, M., Kojima, S., and Uchida, K., *J. Appl. Phys.* 69:7924 (1991).
8. Goodwin, D. G., Glumac, N. G., and Shin, H. S., in *Twenty-Sixth Symposium (International) on Combustion,* The Combustion Institute, Pittsburgh, 1996, pp. 1817–1824.
9. Bertagnolli, K. E. and Lucht, R. P., in *Twenty-Sixth Symposium (International) on Combustion,* The Combustion Institute, Pittsburgh, 1996, pp. 1825–1833.
10. Matsui, Y., Yabe, H., and Hirose, Y., *Jpn. J. Appl. Phys.* 29:1552 (1990).

11. Goodwin, D. G., *Appl. Phys. Lett.* 59:277 (1991).
12. Goodwin, D. G., *J. Appl. Phys.* 74:6895 (1993).
13. Okkerse, M., Klein-Douwel, R. J. H., de Croon, M. H. J. M., Kleijn, C. R., ter Meulen, J. J., Marin, G. B., and van den Akker, H. E. A., in *Chemical Vapour Deposition Proceedings of the Fourteenth International Conference and EUROCVD-11* (M.D. Allendorf et al., eds.), Electrochemical Society, 1997, p. 163.
14. Okkerse, M., private communication, 1997.
15. Klein-Douwel, R. J. H., Spaanjaars, J. J. L., and ter Meulen, J. J., *J. Appl. Phys.* 78:2086 (1995).
16. Klein-Douwel, R. J. H., Schermer, J. J., and ter Meulen, J. J., *Diamond Rel. Mater.* 7:1118 (1998).
17. Klein-Douwel, R. J. H. and ter Meulen, J. J., *J. Appl. Phys.* 83:4734 (1998).
18. Schermer, J. J., Elst, W. A. L. M., and Giling, L. J., *Diamond Rel. Mater.* 4:1113 (1995).
19. Frenklach, M. and Spear, K. E., *J. Mater. Res.* 3:133 (1988).
20. Frenklach, M., *J. Appl. Phys.* 65:5142 (1989).
21. Frenklach, M. and Wang, H., *Phys. Rev. B* 43:1520 (1991).
22. Harris, S. J. and Goodwin, D. G., *J. Phys. Chem.* 97:23 (1993).
23. Gruen, D. M., Liu, S., Krauss, A. R., Luo, J., and Pan, X., *Appl. Phys. Lett.* 64:1502 (1994).
24. Gruen, D. M., Zuiker, C. D., Krauss, A. R., and Pan, X., *J. Vac. Sci. Technol. A* 13:1628 (1995).
25. Redfern, P. C., Horner, D. A., Curtiss, L. A., and Gruen, D. M., *J. Phys. Chem.* 100:11654 (1996).
26. Bohr, S., Haubner, R., and Lux, B., *Appl. Phys. Lett.* 68:1075 (1996).
27. Badzian, A., Badzian, T., and Lee, S.-T., *Appl. Phys. Lett.* 62:3432 (1993).
28. Locher, R., Wild, C., Herres, N., Behr, D., and Koidl, P., *Appl. Phys. Lett.* 65:34 (1994).
29. Schermer, J. J. and de Theije, F. K., unpublished.
30. Müller-Sebert, W., Wörner, E., Fuchs, F., Wild, C., and Koidl, P., *Appl. Phys. Lett.* 68:759 (1996).
31. Jin, S. and Moustakas, T. D., *Appl. Phys. Lett.* 65:403 (1994).
32. Cao, G. Z., Schermer, J. J., van Enckevort, W. J. P., Elst, W. A. L. M., and Giling, L. J., *J. Appl. Phys.* 79:1357 (1996).

COMMENTS

J. Gore, Purdue University, USA. What are the solid-surface temperatures during diamond growth?

Author's Reply. The surface temperature of the molybdenum substrate is kept constant at 1050 °C by water cooling (sprayed from below). The resulting temperature of the diamond surface is about 150° higher, or about 1200 °C (as determined from two-color pyrometry measurements in a similar setup).

•

David R. Crosley, SRI International, USA.

1. You said you detected H atoms via a Balmer line. Were you measuring excited state atoms, and how did that relate to the ground-state concentration?
2. In one slide, you showed C_2 at two different positions of the flame from the substrate. The units were just given in counts. How did the actual concentrations scale?
3. If you had a profile of growth rate at the same position you measured each species, you could just about fit it to $a^*[C_2] + b^*[CN] + c^*[H]$. Did you try that?

Author's Reply.

1. Maybe I was not clear enough about our measuring method: We excite ground-state H atoms via a two-photon transition (2×205 nm) to the $n = 3$ level, from which fluorescence to the $n = 2$ level (Balmer line) follows, which is detected with the CCD camera.
2. Because we did not determine absolute concentrations, but only relative concentrations, this cannot be answered exactly. Relative concentrations very close to the substrate (in a plane about 0.1 mm above the substrate) have been determined and are shown in the horizontal profiles. These can be compared because the temperature in this region is not expected to vary much, a fact that has been confirmed by simultaneously measuring C_2 excitation spectra in this plane at various distances from the flame axis.
3. No, we did not try that. Because there are more species present above the substrate than the three mentioned and because the role of all present species is not yet (fully) understood, the fitting formula you mentioned is most likely not very meaningful.